Energy Consumption Optimization for UAV Base Stations with Wind Compensation

Marek Ruzicka, Zdenek Becvar, *Senior Member, IEEE*, Juraj Gazda

***Abstract*—In this letter, an energy-efficient algorithm for positioning of unmanned aerial vehicle-based base stations (UAV-BSs) is presented. The objective is to reduce the propulsion power consumption of UAV-BSs while not compromising the communication capacity of user equipments (UEs). As a significant step beyond state-of-the-art, we consider an effect of wind. To this end, we develop a new model of a propulsion energy consumption for the UAV-BSs reflecting an impact of wind. Furthermore, we propose a novel algorithm based on an ensemble learning optimizing the 3D trajectory of UAV-BSs over time in realistic environment with wind to reduce the propulsion energy consumption. The results show that the proposed approach reduces the propulsion energy consumption of UAV-BSs by up to 47% with only a negligible degradation in the UEs capacity compared to state-of-the-art works.**

***Index Terms*—UAV base station, energy consumption, wind, modeling, ensemble learning, machine learning**

I. Introduction

The base stations mounted on unmanned aerial vehicles (UAV-BSs) represent a promising solutions offering a connectivity to user equipments (UEs) during emergency or temporary peak traffic conditions. The major limitation related to a deployment of the UAV-BS is the battery capacity and, consequently, operational time. The available battery capacity is shared by communication (transmission power), and flying (propulsion power).

Solutions targeting to reduce the transmission power of UAV-BSs typically aim to determine positions of the UAV-BSs. For example, in [1], the authors propose the optimal UAV-BSs positioning based on the circle placement problem to maximize the number of covered UEs. Furthermore, successive convex approximation for the UAV-BS deployment considering different transmission power allocated to the UEs is adopted in [2]. Downlink power control for a fleet of UAV-BSs is considered in [3]. In practical deployment of the rotary-wing UAV-BSs, the transmission power consumption is few orders of magnitude lower than the propulsion power consumption [4]. Hence, the transmission power is commonly neglected and the propulsion power optimization is a key challenge.

The propulsion power optimization is addressed, e.g., in [5], [6], where a closed form solution for the UAV-BS trajectory is derived. Then, in [7], the energy consumption and trajectory design, considering the UAV's dynamics and UAV's turning angles, are optimized. In [8], the authors adopt multi-agent reinforcement learning to solve a multi-criteria optimization problem involving the propulsion power reduction. Finally, joint optimization of the UAV trajectory and beamforming under a stochastic wind uncertainty is delivered in [9]. Nevertheless, up to our best knowledge, there is no work that would take advantage of the wind flow distribution on the UAV-BS trajectory design and corresponding effects on the UAV-BS's propulsion energy. Hence, in this paper, we minimize the propulsion energy consumption of the UAV-BSs serving stationary/slowly moving UEs while taking the efect of wind on the energy consumption of the UAV-BS into account.

The major contributions of our work are summarized as follows. First, we propose the UAV-BS energy consumption model in the presence of wind considering: *i)* the wind speed and wind direction, *ii)* the UAV-BS physical configuration, and *iii)* instantaneous UAV-BS velocity. Second, we predict the sub-optimal trajectory, defined by the circle center, altitude, and flight radius, minimizing the propulsion energy consumption and leveraging the wind via ensemble learning. As shown in [5], hovering with (close to) zero speed results in a significant propulsion energy consumption. Hence, the circular trajectory is commonly considered due to complexity and practical limitations on maneuvering of the UAVs, see, e.g. [5], [10]. Last, we demonstrate a significant propulsion energy saving reached by our proposed algorithm at the cost of only a negligible capacity degradation compared to the state-of-the-art algorithm maximizing the capacity.

II. System model

In this section, we introduce a generic model of the system, communication model, and wind flow model.

A. Generic model of the system and environment

We consider 3D urban area $\mathcal{A} \subset \mathbb{R}^3$ with buildings. The buildings occupy an area defined by coordinates $\mathcal{A}'$. Furthermore, N UEs are deployed at locations $\mathcal{U} = \{\mathbf{u}_1, \mathbf{u}_2, ..., \mathbf{u}_N\}$, where $\mathbf{u}_n = [x_n, y_n, z_n] \in \mathcal{A}^{\text{o}}, \forall n \in \langle 1, N \rangle$ and $\mathcal{A}^{\text{o}} = \mathcal{A} - \mathcal{A}'$ represents the area, where the UEs and the

Manuscript received Fe XX, 2022; revised September XX, 2022. This work was supported in part by APVV, project numbers APVV-18-0214 and APVV-SK-CZ-RD-21-0028, project ITMS2014+: 313011V422, by the European Regional Development Fund, and by the Ministry of Education, Youth and Sports, Czech Republic, under Grant LTT20004.

Marek Ruzicka and Juraj Gazda are with Technical University of Kosice, Department of Computers and Informatics, Slovakia (e-mail: marek.ruzicka@tuke.sk, juraj.gazda@tuke.sk)

Zdenek Becvar is with Czech Technical University in Prague, Faculty of Electrical Engineering, Technicka 2, 16627 Prague, Czech Republic (e-mail: zdenek.becvar@fel.cvut.cz)

UAV-BSs can move. There are also M static base stations (SBSs) located on the rooftops of the buildings at coordinates $\mathcal{S} = \{\mathbf{s}_1, \mathbf{s}_2, ..., \mathbf{s}_M\}$, where $\mathbf{s}_m = [x_m, y_m, z_m] \in \mathcal{A}', \forall m \in \langle 1, M \rangle$. Moreover, K UAV-BSs relaying data from the SBSs to the UEs are also deployed in the area at coordinates $\mathcal{D}(t) = \{\mathbf{d}_1(t), \mathbf{d}_2(t), ..., \mathbf{d}_K(t)\}$, where $\mathbf{d}_k(t) = [x_k(t), y_k(t), z_k(t)] \in \mathcal{A}^{\mathrm{o}}, \forall k \in \langle 1, K \rangle$ at the time t.

Realistic UAV-BSs are limited in maneuvering and their movement should be smooth in terms of direction changes to avoid a high energy consumption [5]. Therefore, we design the circular trajectory, which approximates the optimal trajectory sufficiently with only a minor impact on the performance as demonstrated in [11]. Moreover, a minor deviation in the position of UAV-BSs with respect to an optimal generic shape of the trajectory has only a marginal impact on the capacity of UEs [12]. We consider the circular trajectory with radii $\mathbf{r} = [r_1, r_2, ...r_K]$ at the circle centers $\mathbf{F} = [\mathbf{f}_1, \mathbf{f}_2, \ldots, \mathbf{f}_K] \in \mathcal{R}^{K \times 3}$, where $\mathbf{f}_k = [f_{k,\mathrm{x}}, f_{k,\mathrm{y}}, f_{k,\mathrm{z}}]$. The position of the k-th UAV-BS at the time t is, then, defined as $\mathbf{d}_k(t) = [f_{k,\mathrm{x}} - r_k * \cos\alpha(t), f_{k,\mathrm{y}} - r_k * \sin\alpha(t), f_{k,\mathrm{z}}]$, where $\alpha(t)$ is the relative angle of the UAV-BS to the x-axis.

B. Communication models

We consider orthogonal downlink transmission to the UEs. The capacity of the access channel (superscript a) between the k-th UAV-BS and the associated n-th UE is expressed as

$$C^{\mathrm{a}}_{k,n} = B_n \log_2 \left(1 + \frac{P^{\mathrm{Tx}}_{k,n} g^{\mathrm{a}}_{k,n} \theta^{\mathrm{a}}_{k,n}}{B_n \sigma^2 + I}\right), \tag{1}$$

where B_n is bandwidth associated to n-th UE. The available bandwidth of k-th UAV-BS is distributed equally among its associated UEs. The parameter $P^{\mathrm{Tx}}_{k,n}$ is the transmission power of the k-th UAV-BS associated to the n-th UE, $g^{\mathrm{a}}_{k,n}$ represents the access channel gain between the k-th UAV-BS and the n-th UE, $\theta^{\mathrm{a}}_{k,n}$ denotes the fading, σ^2 represents the noise power density, and I is the interference from neighboring cells.

Analogously, the capacity of the backhaul channel (superscript b) between the m-th SBS and the k-th UAV-BS required for transmission of data of the n-th UE is defined as

$$C^{\mathrm{b}}_{m,k} = B_n \log_2 \left(1 + \frac{P^{\mathrm{Tx}}_{m} g^{\mathrm{b}}_{m,k} \theta^{\mathrm{b}}_{m,k}}{B_n \sigma^2 + I}\right), \tag{2}$$

where P^{Tx}_{m} is the transmission power of the m-th SBS, $g^{\mathrm{b}}_{m,k}$ is the backhaul channel gain between the m-th SBS and the k-th UAV-BS. Since the bandwidth allocation does not affect the UAV-BS's propulsion energy consumption, we assume equal B_n allocated for all UEs served by the same UAV-BS.

For the UAV-BSs' communication, half-duplex decode-and-forward transmission is adopted. Hence, the capacity of the channel between the m-th SBS and the n-th UE via the k-th UAV-BS is determined as

$$C_{m,k,n} = \min(T^{\mathrm{b}}_n C^{\mathrm{b}}_{m,k}, (1 - T^{\mathrm{b}}_n) C^{\mathrm{a}}_{k,n}), \tag{3}$$

where $T^{\mathrm{b}}_n \in [0, 1]$ is the normalized time scheduled for the n-th UE transmission over the backhaul, and $(1 - T^{\mathrm{b}}_n)$ is the normalized time for the access channel transmission. To avoid a bottleneck on either of these channels, for the k-th UAV forwarding data from the m-th SBS, we assume [13]

$$\sum_{n=1}^{N} T^{\mathrm{b}}_n C^{\mathrm{b}}_{m,k} = \sum_{n=1}^{N} (1 - T^{\mathrm{b}}_n) C^{\mathrm{a}}_{k,n}. \tag{4}$$

C. Wind flow model

We model the dynamic effects of the wind via a generally recognized k-ε model based on the Reynolds Averaged Navier-Stokes (RANS) equations [14]. The k-ε model considers the turbulent wind flow, which is present in an urban environment with multiple obstacles in the wind path and uses time-averaged equations of motion for wind. In practice, the model of the environment is described through the finite volume method (FVM) using a mesh, which represents a geometry of the environment. The accuracy of the model is determined via a sensitivity of the mesh and a number of iterations [15]. The mesh should be sensitive enough to capture the geometry of the model sufficiently. However, too sensitive mesh leads to a high computational complexity. The number of iterations determines how many times the model runs until convergence to a correct prediction of wind. The mesh is created either manually or by a tool, e.g., based on UAV scanning the selected area. The mesh is then projected into a virtual wind tunnel and simultaneously, an inlet and an outlet, representing a side from which the wind flows inside and outside the tunnel, are selected. The wind velocity on inlet $\vec{I} = [i_{\mathrm{x}}, i_{\mathrm{y}}, i_{\mathrm{z}}]$, and turbulent intensity and viscosity are measured at a given reference point (RP), e.g., a weather station on a building, and inserted to the model.

The k-ε model provides an information about the wind velocity $\vec{w_a} = [w_{\mathrm{x}}, w_{\mathrm{y}}, w_{\mathrm{z}}]$ for each discrete position $a \in \mathcal{A}^{\mathrm{o}}$. Time evolution of the wind velocity vectors is expressed as the time evolution of mean velocity vector field (flow velocity) from the left side of the convective form of the RANS equations, as defined in [14]. The length of UAV-BS operational time ($\sim$ minutes) is sufficiently large compared to the time-scale of turbulence in the wind flow ($\sim$ milliseconds). Hence, we can take an advantage of the wind-flow averaged values from RANS for the design of the UAV-BS trajectory instead of the instantaneous wind values, which are affected by difficult to estimate small-scale turbulence in practice [14].

III. Model of UAV energy consumption with wind

In this section, we introduce a novel model of the propulsion energy consumption for the UAV-BS considering wind.

To derive a model suitable for the wind condition, let us start with the model for the propulsion power consumed at the speed $\tilde{V}$ *without wind*, as introduced in [6].

$$P(\tilde{V}) = \underbrace{P_0 \left(1 + \frac{3\tilde{V}^2}{V^2_{\mathrm{tip}}}\right)}_{\text{blade profile}} + \underbrace{P_{\mathrm{i}} \left(\sqrt{1 + \frac{\tilde{V}^4}{4v_0^4}} - \frac{\tilde{V}^2}{2v_0^2}\right)^{1/2}}_{\text{induced}} + \underbrace{\frac{1}{2} d_0 \rho s A \tilde{V}^3}_{\text{parasite}}, \tag{5}$$

where P_0, P_i, d_0, and s are the UAV hardware specific constants (see [6]), ρ defines the air density, $V_{\text{tip}} = R\omega$ is the tip speed of the rotor blade for the blade angular speed ω and the rotor radius R, v_0 represents the rotor speed induced by forward flight, and A is the rotor disc area [6].

Note that this model is significantly extended towards a consideration of the dynamics of the UAVs for practical realizations in [7]. The models in both [6], [7] lead to similar trends in the energy consumption with respect to the UAV speed, see [7]. Moreover, none of these two models considers wind and its impact on the energy, however, a generic principle of an extension to include wind is analogical for both. As the model from [6] is of much lower complexity than the model in [7] and an integration of wind is easier to be illustrated on the model in [6], we focus on this model, and we include wind-related motion factors into this model in the following way.

Generally, the wind force F_{w} actuating on an effective surface A_{w} of the UAV is calculated as $F_{\text{w}} = \frac{1}{2}\rho w^2 A_{\text{w}}$. The effective surface A_{w} is the total surface hit by respective air flow. Besides, the air resistance force acting in an opposite direction of the flight is calculated as $F_{\text{V}} = \frac{1}{2}\rho V^2 A_{\text{V}}$ actuating on effective surface A_{V}.

We assume the wind velocity $\vec{w} = w_{\text{x}}\vec{e}_{\text{x}} + w_{\text{y}}\vec{e}_{\text{y}} + w_{\text{z}}\vec{e}_{\text{z}}$ expressed by means of the orthogonal unit vectors $\vec{e}_{\text{x}}, \vec{e}_{\text{y}}, \vec{e}_{\text{z}}$ representing the components of speed in each axis. By analogy, we suppose that the speed of the UAV in the system related to a ground-based observer is $\vec{V} = V_{\text{x}}\vec{e}_{\text{x}} + V_{\text{y}}\vec{e}_{\text{y}} + V_{\text{z}}\vec{e}_{\text{z}}$. Exploiting the components of the wind velocity, we can compute the x component of the wind force $\vec{F}^{\text{w}}$ as $\vec{F}^{\text{w}}_{\text{x}} = \frac{1}{2}\rho w_{\text{x}} w A_{\text{w}}\vec{e}_{\text{x}}$. $\vec{F}^{\text{w}}_{\text{y}}$ and $\vec{F}^{\text{w}}_{\text{z}}$ are computed analogically. The air resistance force $\vec{F}^{\text{V}}$ consisting of $\vec{F}^{\text{V}}_{\text{x}}, \vec{F}^{\text{V}}_{\text{y}}$, and $\vec{F}^{\text{V}}_{\text{z}}$ is computed correspondingly from $\vec{V}$ and A_V. The final force actuating on the UAV is a sum of components of $\vec{F}^{\text{V}}$ and $\vec{F}^{\text{w}}$, thus $\vec{F} = \vec{F}^{\text{V}} + \vec{F}^{\text{w}}$. The considered model is depicted in Fig. 1.

The total propulsion energy of the k-th UAV-BS $E_k = E^{\text{p}}_k + E^{\text{air}}_k$ is the sum of: *i)* the energy E^{p}_k corresponding to the k-th UAV power required to maintain motion at the speed V_k for the total flight time τ, and *ii)* dissipated energy E^{air}_k due to the air flow related force $\vec{F}_k$ actuating on the surfaces of the k-th UAV. Both components of the total propulsion energy consumption are computed by time integration of the related variables, i.e., $E^{\text{p}}_k = \int_0^\tau dt P(V_k)$, $E^{\text{air}}_k = \int_0^\tau dt \vec{F}_k(t) \cdot (\frac{d\vec{s_k}(t)}{dt})$, where $\vec{s_k}(t)$ represents the pathway projection of k-th UAV in space.

IV. Problem Formulation

The objective is to minimize the propulsion energy consumption of the UAV-BSs via a determination of the UAV-BS trajectories. Due to real-world limitations imposed on the trajectories, as explained in Section II, our goal is to determine the circular trajectories including their centers; $\mathbf{F}^* = [\mathbf{f}^*_1, \mathbf{f}^*_2, \dots \mathbf{f}^*_K]$ for all UAV-BSs and respective radii $\mathbf{r}^* = [r^*_1, r^*_2, ..., r^*_K]$. The energy saving optimization problem is, thus, defined as

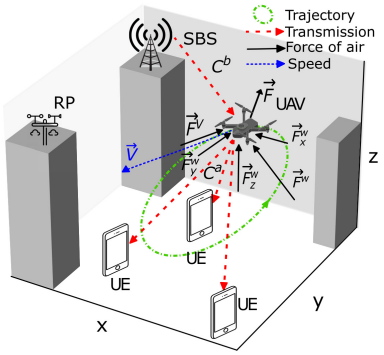

Fig. 1. Model showing forces actuating on UAV-BS and speed vector, trajectory, and backhaul/access channels of UAV-BS.

$$\mathbf{F}^*, \mathbf{r}^* = \underset{\mathbf{F},\mathbf{r}}{\operatorname{argmin}} \sum_{k=1}^{K} E_k, \tag{6}$$

$$\text{s.t. } (\mathbf{f}^*_k) \in \mathcal{A}^{\text{o}}, \qquad \forall k \in \langle 1, K\rangle \tag{a}$$

$$f^*_{k,z} \in \langle z_{\min}, z_{\max}\rangle, \quad \forall k \in \langle 1, K\rangle \tag{b}$$

$$r^*_k \in \langle r_{\min}, r_{\max}\rangle, \quad \forall k \in \langle 1, K\rangle \tag{c}$$

$$C_{m,k,n}(d_k(t)) \geq (1-\gamma)C'_{m,k,n}, \forall k \in \langle 1, K\rangle, \quad \forall m \in \langle 1, M\rangle, \forall n \in \langle 1, N\rangle. \tag{d}$$

The constraint (a) defines the set of all possible locations $\mathcal{A}^{\text{o}}$ in the area excluding buildings and obstacles, where the presence of UAV-BSs is not allowed. The constraint (b) defines the range of possible UAV-BS altitudes and the constraint (c) defines the range of possible flight radii. The constraint (d) ensures that the capacity $C_{m,k,n}$ of the n-th UE associated to the m-th SBS via the k-th UAV at the position d_k at the time t does not drop below $(1-\gamma)C'_{m,k,n}$, where γ represents the maximum relative allowed decrease in the capacity of UEs with respect to the maximized capacity $C'_{m,k,n}$ of the n-th UE neglecting the energy consumption. Hence, the constraint (d) ensures the capacity degradation is negligible.

The optimization problem in (6) is NP-hard nonconvex non-linear programming problem with embedded numerical evaluation of partial differential equations represented by the RANS with linear constraints on the variables using FVM. The time complexity of the FVM is $\mathcal{O}(\eta \log(\eta))$, where η is the mesh sensitivity characterizing the FVM environment. The FVM approximates values by a time evaluation in ψ discrete time steps, so the complexity becomes $\mathcal{O}(\eta \log(\eta)\psi)$ [15]. The cost function in (6) is, thus, extremely computationally expensive. Hence, we adopt machine learning to make the solution feasible for practical applications.

V. Proposed Solution for UAV-BS Trajectory Design with Wind Consideration

In this section, we first determine the theoretical minimum energy consumption. Then, we propose a solution to problem (6). The solution is based on the ensemble learning adopted to predict the sub-optimal energy efficient positions of the UAV-BSs $\overline{\mathbf{F}}$ and respective radii $\overline{\mathbf{r}}$. We take advantage of the wind

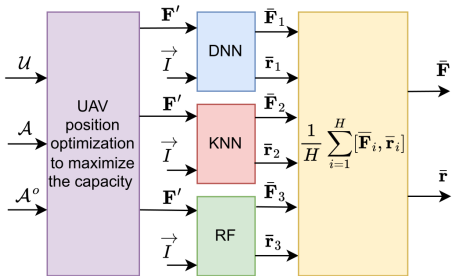

Fig. 2. Ensemble learning approach to determine energy-efficient UAV-BS trajectory. Three base learners (DNN, KNN, RF) are fed with capacity-maximizing UAV-BSs' positions $\mathbf{F}'$ and wind information $\vec{I}$ at the RP.

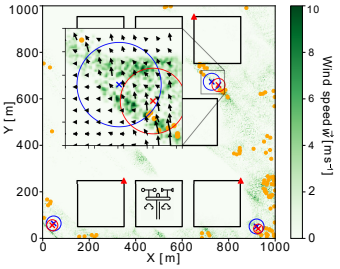

Fig. 3. Example of simulation setup with buildings (black squares), UEs positions (orange dots), SBS positions (red triangles), reference point (RP), capacity-max positions of UAV-BSs derived according to [17] (red crosses and circle trajectory) and UAV-BSs positions computed by the proposed approach (blue crosses and circle trajectory). The wind speed velocity is represented by the green heatmap with zoomed detail encompassing average wind speed vectors at given positions. Note that z-axis omitted for clarity.

distribution in the area and we search for a trajectory, where a head wind is as low as possible, while a tail wind is as high as possible to reduce the energy consumption.

To identify the theoretical minimum energy consumption of UAV-BSs as defined in (6), we adopt the exhaustive search deriving the optimum $\mathbf{F}^*$ and $\mathbf{r}^*$ by testing all possible options of the UAV-BSs deployment (taking the constraints a, b, and c into account) and selecting the one leading to the minimum energy consumption while fulfilling the capacity constraint d. For practical applications, the exhaustive search is not feasible due to a huge computational complexity. Thus, we also solve (6) as the prediction problem via ensemble learning, where $\mathbf{F}^*$ and $\mathbf{r}^*$ are used only as the targets in the training phase and their computation online is not required.

The ensemble learning combines several base learners to improve prediction performance in regression problems compared to standalone predictors. We adopt the heterogeneous set of learners $\mathcal{F}_o = \hat{f}_i$, $i = \{1, 2, \ldots, H\}$, where $H = 3$, as shown in Fig. 2. In the proposed solution, we use a deep neural network (DNN) in combination with traditional random forests (RF) and K-nearest neighbors (KNN) to build heterogeneous ensemble enjoying the benefits of a lower computation cost (shallow DNN and relatively low computing requirements of RF and KNN) and higher diversity potentially leading to a performance improvement [16]. Besides, the individual base learners are characterized by a high sensitivity to the dataset samples and even small changes in the training samples could result in large changes in the predicted output in our problem. However, when combined into the ensemble learning, the resulting error is lower than that of the single classifier [16].

The feature vector for the ensemble learning is identical for all three base learners and consists of $\mathbf{F}'$, determined via any existing algorithm for positioning of the UAV-BSs to maximize the capacity, and wind information at the RP $\vec{I} = [i_\mathrm{x}, i_\mathrm{y}, i_\mathrm{z}]$. At the deployment stage, the ensemble output is implemented as the average of base learners, i.e., $[\bar{\mathbf{F}}, \bar{\mathbf{r}}] = \frac{1}{H}\sum_{i\in\mathcal{F}} \hat{f}_i[\mathbf{F}', \vec{I}]$.

The hyperparameters of the base learners are identified using the grid-search optimization. The DNN predictor consists of three hidden layers with 30, 40, and 40 neurons respectively, employing ReLU activation function. RF reaches the highest performance, when the number of estimators is set to 160 and the maximum depth equals to 13. For the KNN, the number of neighbors is set to the number of UEs N divided by a desired number of UAV-BSs K.

VI. Performance Analysis

In our simulation setup, we consider a rectangular urban area with a size of 1×1 km with 8 buildings of different heights. We consider five SBSs located in random positions on the buildings. The UEs are located randomly following the Binomial point distribution. We consider $B = 20$ MHz and spectral density of noise of -174 dBm/Hz. The transmission powers of the SBS and the UAV-BS are equal to 46 dBm and 30 dBm, respectively. Path loss model for line of sight (LoS) channels is in line with [17]. For non-LoS channels, an attenuation of walls/obstacles is added on the top of LoS attenuation as in [17]. Fast fading components are generated as exponentially distributed random variables with unit mean. The simulation outputs are averaged out over 10 000 runs.

The exhaustive search to determine the minimum energy consumption is performed in a discrete space with a step size of 1 m. Finally, the capacity deterioration parameter introduced in (6*d*) is set to $\gamma = 0.03$.

We consider the UAV-BSs represented by the DJI spreading wings S900 model with the shape and HW characteristics given in the specification manual[1]. The visualization of the area considered in our simulation setup is given in Fig. 3.

We compare performance of our proposal with two baseline schemes: *i)* exhaustive search (labeled as *lower-bound*) providing $\mathbf{F}^*$ and $\mathbf{r}^*$, and *ii)* state-of-the-art algorithm maximizing capacity using DNN, as proposed in [17] (labeled as *capacity-max*). Note that the *capacity-max* algorithm does not account for the wind effect in the trajectory design.

As the performance metrics, we adopt the time averaged propulsion energy consumption $E = \frac{1}{\tau}E_k^\mathrm{p}$ and the average sum capacity defined as time averaged sum of all UEs capacities, i.e. $C = \frac{1}{\tau}\int_0^\tau dt \sum_{m=1}^{M}\sum_{k=1}^{K}\sum_{n=1}^{N}(C_{m,k,n}(\mathbf{d}_k(t)))$.

Fig. 4a shows energy savings of 47% introduced by the proposed approach with respect to the *capacity-max* solution for the average wind speed $|\vec{w}| = 10$ ms^{-1} disregarding the number of UEs deployed in the system. Such savings are expected, since the *capacity-max* does not consider wind in the trajectory design and, hence, the UAV-BSs copes with potentially strong wind during flight. The standalone base

[1] http://dl.djicdn.com/downloads/s900/en/S900_User_Manual_v1.2_en.pdf

learners show a slight performance degradation compared to the proposed approach. Hence, a diversity among the base learners results in a superior performance of the proposed ensemble learning. In Fig. 4b, we plot the average sum capacity vs. number of UEs deployed in the system for the average wind speed $|\overline{\vec{w}}| = 10$ ms^{-1}. The proposed solution almost matches the performance of the *capacity-max* algorithm (loss below 0.3%) disregarding the number of UEs. The standalone base learners show a bit larger performance degradation of about 1.2%, 1.4%, and 2% for DNN, KNN, and RF, respectively.

In Fig. 5a, we show the average propulsion energy consumption over the varying wind speed. The *capacity-max* algorithm with no wind compensation is characterized by an increasing energy consumption with the wind speed. Contrary, our proposed approach and base learners take advantage of the turbulent wind flows by adjusting the trajectories resulting in a decreasing energy consumption with an increasing wind speed. The reduced energy consumption for stronger wind is the result of the optimized UAV-BS trajectory considering the wind strength at different locations so that the UAV-BS follows trajectory with a strong tail wind and weak head wind. The energy saving by our proposal with respect to the state-of-the-art *capacity-max* algorithm achieves 47% energy savings for the wind speed $|\overline{\vec{w}}| = 10$ ms^{-1}. Besides, the proposal provides almost identical performance as the computationally complex *lower-bound* with difference always below 2%. The energy consumption of the base learners is up to 8% worse compared to the ensemble learning. Finally, in Fig. 5b, we observe the proposed algorithm almost matches (difference below 0.1%) the sum capacity of the *lower-bound* and *capacity-max* across all investigated wind speed characteristics. The base learners show a larger deterioration between 1.37 and 2.75%.

VII. Conclusions

We have introduced new analytical model of the UAV-BS propulsion energy consumption taking the wind into account in order to express the energy consumption at the presence of the turbulent wind flows. Furthermore, we have proposed a novel 3D positioning of UAV-BSs leveraging the wind flow distribution to reduce the propulsion energy consumption. The proposed solution is based on the ensemble learning consisting of three base learners. The simulations show that the proposal reduces the energy consumption significantly (up to 47%) while the sum-capacity is deteriorated only negligibly compared to the state-of-the-art work neglecting the wind.

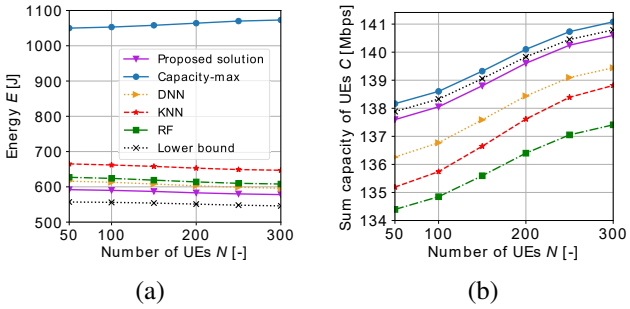

(a) (b)

Fig. 4. Average energy consumption (subplot a) and sum-capacity (subplot b) over varying number of UEs.

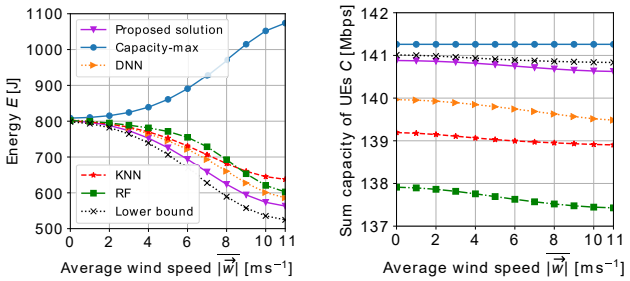

(a) (b)

Fig. 5. Average energy consumption (subplot a) and sum capacity (subplot b) as a function of the average wind speed.

References

[1] M. Alzenad, A. El-Keyi, F. Lagum, and H. Yanikomeroglu, "3-D placement of an unmanned aerial vehicle base station (UAV-BS) for energy-efficient maximal coverage," *IEEE Wireless Communications Letters*, vol. 6, no. 4, pp. 434–437, 2017.

[2] L. Wang, B. Hu, and S. Chen, "Energy efficient placement of a drone base station for minimum required transmit power," *IEEE Wireless Communications Letters*, vol. 9, no. 12, pp. 2010–2014, 2020.

[3] L. Li, Q. Cheng, K. Xue, C. Yang, and Z. Han, "Downlink transmit power control in ultra-dense UAV network based on mean field game and deep reinforcement learning," *IEEE Transactions on Vehicular Technology*, vol. 69, no. 12, pp. 15 594–15 605, 2020.

[4] C. Di Franco and G. Buttazzo, "Energy-aware coverage path planning of UAVs," in *2015 IEEE international conference on autonomous robot systems and competitions*. IEEE, 2015, pp. 111–117.

[5] Y. Zeng and R. Zhang, "Energy-efficient UAV communication with trajectory optimization," *IEEE Transactions on Wireless Communications*, vol. 16, no. 6, pp. 3747–3760, 2017.

[6] Y. Zeng, J. Xu, and R. Zhang, "Energy minimization for wireless communication with rotary-wing UAV," *IEEE Transactions on Wireless Communications*, vol. 18, no. 4, pp. 2329–2345, 2019.

[7] B. Li, Q. Li, Y. Zeng, Y. Rong, and R. Zhang, "3D trajectory optimization for energy-efficient UAV communication: A control design perspective," *IEEE Transactions on Wireless Communications*, 2021.

[8] Y. Yu, J. Tang, J. Huang, X. Zhang, D. K. C. So, and K.-K. Wong, "Multi-objective optimization for UAV-assisted wireless powered IoT networks based on extended DDPG algorithm," *IEEE Transactions on Communications*, vol. 69, no. 9, pp. 6361–6374, 2021.

[9] D. Xu, Y. Sun, D. W. K. Ng, and R. Schober, "Multiuser MISO UAV communications in uncertain environments with no-fly zones: Robust trajectory and resource allocation design," *IEEE Transactions on Communications*, vol. 68, no. 5, pp. 3153–3172, 2020.

[10] P. Beigi, M. S. Rajabi, and S. Aghakhani, "An overview of drone energy consumption factors and models," *arXiv:2206.10775*, 2022.

[11] M. Yang, S.-W. Jeon, and D. K. Kim, "Optimal trajectory for curvature-constrained UAV mobile base stations," *IEEE Wireless Communications Letters*, vol. 9, no. 7, pp. 1056–1059, 2020.

[12] Z. Becvar, M. Nikooroo, and P. Mach, "On energy consumption of airship-based flying base stations serving mobile users," *IEEE Transactions on Communications*, 2022.

[13] M. K. Shehzad, A. Ahmad, S. A. Hassan, and H. Jung, "Backhaul-aware intelligent positioning of UAVs and association of terrestrial base stations for fronthaul connectivity," *IEEE Transactions on Network Science and Engineering*, vol. 8, no. 4, pp. 2742–2755, 2021.

[14] T. Kajishima and K. Taira, "Reynolds-Averaged Navier–Stokes Equations," in *Computational Fluid Dynamics*. Springer, 2017, pp. 237–268.

[15] J. Yang, T. Michael, S. Bhushan, A. Hanaoka, Z. Wang, and F. Stern, "Motion prediction using wall-resolved and wall-modeled approaches on a Cartesian grid," in *Proc. of the 28th Symposium on Naval Hydrodynamics (USA, Pasadena)*. Citeseer, 2010.

[16] M. A. Ganaie, M. Hu *et al.*, "Ensemble deep learning: A review," *arXiv preprint arXiv:2104.02395*, 2021.

[17] M. Najla, Z. Becvar, P. Mach, and D. Gesbert, "Positioning and association rules for transparent flying relay stations," *IEEE Wireless Communications Letters*, vol. 10, no. 6, pp. 1276–1280, 2021.